Fusion of registered 2D intensity and 3D range data: application to the differential light absorption technique

Jean-François Méthot and Denis Poussart

Computer Vision and Digital Systems Laboratory Department of
Electrical Engineering Laval University, Quebec, CANADA, G1K 7P4

Abstract

The present work outlines a design strategy whereby 2D intensity and 3D range data are fused in order to yield higher accuracy range sensing. The fusion algorithm described here is applied to the differential light absorption (DLA) range finder technique. This technique is well suited for small object that may be immersed in a colored liquid. The observation that an intensity image is available as part of the 3D acquisition process suggests that sensory fusion may be used in order to increase the range accuracy. The bulk of the processing operations are fully amenable to parallelism and have been mapped on a massively parallel SIMD machine. The improvement obtained for the range image has been evaluated for a variety of 3D scenes, and is typically better than 2 bits.

1. Introduction

The present work outlines a design strategy whereby registered 2D intensity and 3D range data are fused in order to yield higher performance range sensing, thus improving the precision and reliability of 3D range data. The fusion algorithm described here is applied to the differential light absorption (DLA) range finder technique[1]. This technique is well suited for small objects that may be immersed in a colored liquid. The observation that an intensity image is available as part of the 3D acquisition process suggests that sensory fusion may be used in order to increase the range accuracy. Another motivation for the present approach derives from the general opportunities which may be provided by sensory fusion [2].

The features that is exploited here is that 2D intensity images are generally less noisy than 3D range images. Acquisition of range data may involve intermediate computations and the measurement of more than one parameter, and therefore tends to be subject to larger noise levels. In contrast, technology for intensity data is far more mature, and low noise, wide dynamic range is more readily available. This suggests to combine data from these modalities to transfer some of the precision of the intensity data to the range data.

The organization of the paper is as follows. Section 2 explains the different steps that are required for the general scheme of the fusion method and the specific methods that are addressed in this paper. Section 3 documents the fusion method while Section 4 shows a brief description of the DLA range finder technique. Some results are presented in Section 5.

2. Problem formulation and hypothesis

In order to extract depth information from 2D intensity data, it is necessary to know the reflectance map [4], which contains the combined information of the light distribution and the surface type. Considerable research has been and is being done to recover illuminant direction and surface properties from intensity data or range and intensity data [5, 6].

In general conditions, in order to avoid shadows, it may be reasonable to assume that the illumination of the scene is centered around the axis of camera and that the surface type is homogeneous. Here, we assume that the light sources are far enough away

that a constant illumination and light direction model may be used. We assume that the light source distribution is unknown. We do not consider multiple reflections, the surface reflectance and albedo are assumed constant over the scene. Finally, we do not impose any *a priori* constraint on the object shape.

3. The fusion principle

The fusion framework involves two steps which are illustrated in Figure 1. It assumes that the reflectance map has been measured previously. In the first step, the orientation vectors at each point of the output surface are computed using both input images. In the second step, we compute the output surface from the orientation vectors previously computed using the range image as an initial estimate. Fusion of information is performed in each of the two steps since both images are used. The fusion proceeds iteratively until an appropriate convergence criterion is satisfied.

Step 1: The derivation of range information or spatial orientation from intensity is possible via the image irradiance equation:

$$E(x, y) = \rho R(p, q) \qquad (1)$$

where E represents the recorded intensity, ρ combines the effect of albedo and sources strength and R is the value of the reflectance map. Variables $p = \frac{\partial z}{\partial x}$ and $q = \frac{\partial z}{\partial y}$ are the usual partial derivatives of the range map. E is proportional to the quantity of light reflected by the object to the camera.

A basic issue in the shape-from-shading approach relates to the determination of the direction of local curvature. For all points of the image except singular points, there exist more than one solution to the image irradiance equation. For example, if the light comes from above, Figure 2 shows a set of 12 orientation surfaces that yields the same intensity.

The key idea here is that we have some knowledge of the range values, but they are somewhat noisy. We postulate that the direction of the slope computed over their neighborhood is not so noisy. Therefore, range data is used to estimate local range gradient

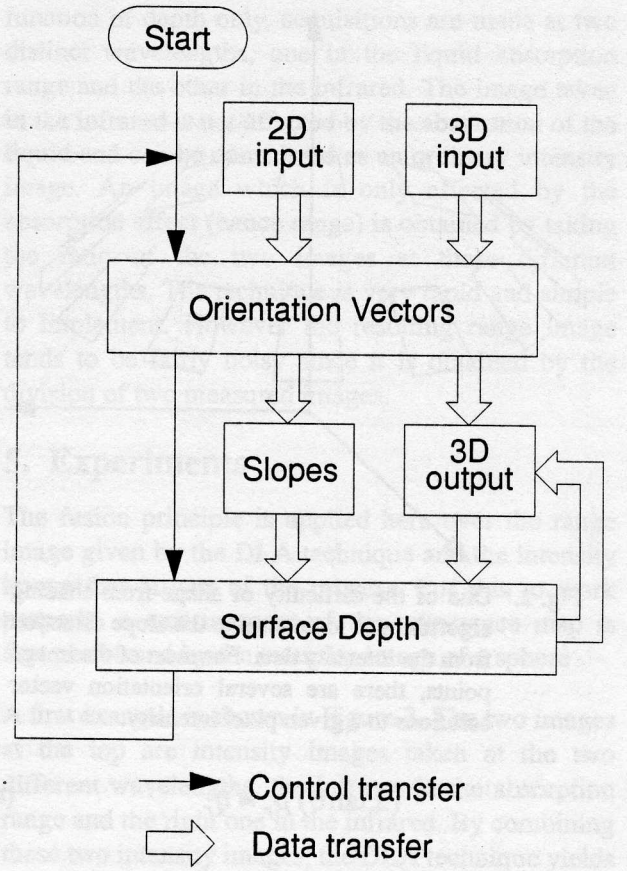

Fig. 1. The fusion framework.

direction. Even if noisy, range data smoothed over a small region provide a close estimation of the range gradient direction. The range gradient direction θ is given by the arctangent of the p_i/q_i ratio computed from the range input image.

$$\theta = \begin{cases} \operatorname{atan}(p_i/q_i) & p_i > 0 \\ \operatorname{atan}(p_i/q_i) + \pi & p_i < 0 \\ \pi/2 & p_i = 0 \quad q_i > 0 \\ -\pi/2 & p_i = 0 \quad q_i < 0 \end{cases} \qquad (2)$$

We know from the measured range image that:

$$(\pm\tan\theta)\, p_i = q_i \qquad (3)$$

So we further assume for the recovered range image that:

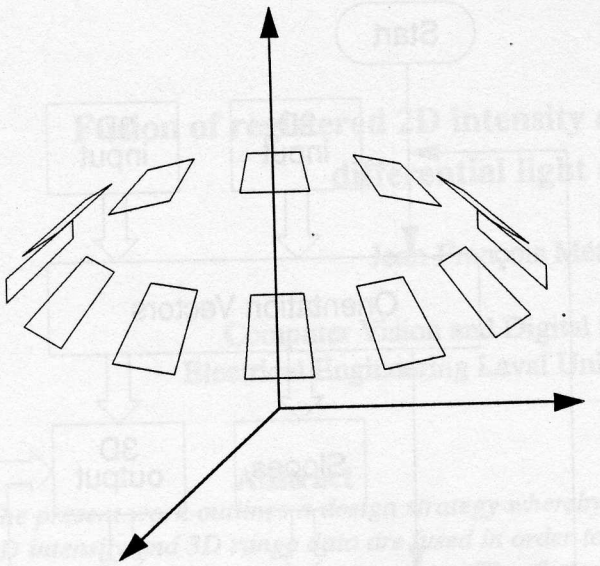

Fig. 2. One of the difficulty of shape-from-shading algorithms is to determine the slope direction from the intensity data. For most of the image points, there are several orientation vector solutions to a given pixel intensity.

$$(\pm\tan\theta)\,\hat{p}_r \approx \hat{q}_r \qquad (4)$$

In the case of the DLA range finder technique, we have to measure or compute the reflectance map. The measurement of a spherical object provides a two dimensional array for the reflectance map. We have to start at the center (p = 0, q = 0) and look in the θ direction by a small step displacement until we reach an intensity value equal to the image value. There, the p and q coordinates represent a new surface orientation estimate $(\hat{p}_r, \hat{q}_r)$.

Step 2: In the second step, the orientation vectors are integrated to yield the output surface. In order to eliminate the non-integrability constraint problem, we resort to an iterative process. This process is defined by minimizing E_d, which represents the distance between the input and output range values, and by minimizing E_p, the distance between $\hat{p}_r$ and $\hat{q}_r$ computed in the first step and their respective values estimated from the output surface. We want the output surface to be close to the range input image for the absolute distance values and we want the surface orientation vectors of this surface to be near those calculated in the first step. The factors α_d and α_p are used to adjust the relative weights of the two terms.

$$E_d = \frac{1}{2}\sum_{i,j\in D} \alpha_d (\hat{z}_{i,j} - d_{i,j})^2 \qquad (5)$$

$$E_p = \frac{1}{2}\sum_{i,j\in D} \alpha_p \Big[\Big(\frac{1}{h_x}(\hat{z}_{i+1,j} - \hat{z}_{i,j}) - \hat{p}_{i,j}\Big)^2 + \Big(\frac{1}{h_y}(\hat{z}_{i,j+1} - \hat{z}_{i,j}) - \hat{q}_{i,j}\Big)^2 \Big] \qquad (6)$$

The input range image is represented by $d_{i,j}$ and the output surface by $\hat{z}$. The variables h_x and h_y are the distance between two pixels in the x and y direction respectively. We want to minimize the sum of the two terms. By setting the derivative of the terms containing $z_{i,j}$ equal to zero, the following iterative scheme is obtained:

$$z_{i,j}^{n+1} = \{\alpha_d d_{i,j} + \alpha_p (z_{i,j+1} + z_{i,j-1} + z_{i+1,j} + z_{i-1,j} + h_x p_{i-1,j} + h_y q_{i,j-1} - h_x p_{i+1,j} - h_y q_{i,j+1})\} / (\alpha_d + 4\alpha_p) \qquad (7)$$

The range value of iteration $n+1$ is given as a function of the range values of the immediate neighbors of iteration n and the local slope estimates. The new depth value is obtained by integrating from the four immediate neighbors toward the center point.

Relaxation: The computation of Step 2 is performed until significant improvements are observed in the range data. An automatic threshold value can be set to determine when to stop iterating. The value of the threshold is given as a function of the changes between the original data and the result after a single iteration. The value of α_1 is the fraction of the change at which the iteration process is to stop.

$$Th_{1,m} = \alpha_1 \sum_{i,j \in D} (z_{i,j}^{1,m} - z_{i,j}^{0,m})^2 \quad (8)$$

The computation of Step 2 ends with iteration n when:

$$\sum_{i,j \in D} (z_{i,j}^{n,m} - z_{i,j}^{n-1,m})^2 \leq Th_{1,m} \quad (9)$$

A global relaxation is then performed by looping back to the first step. Since the first pass has provided an updated estimate of the surface, this may be used to reestimate the range gradient direction and produce improved slope estimates. Each time we loop back at the first step, the last output surface is used as the initial range image. The last output image gives values for Z_m in Equation 2 and to $d_{i,j}$ in Equation 7. The counter variable n represents the iteration of Step 2 and the counter variable m represents the global loop around both steps. A second automatic threshold can be set to determine when to stop the global relaxation around both steps. The value of α_2 is the fraction of the change at which the global process is to stop.

$$Th_2 = \alpha_2 \sum_{i,j \in D} (z_{i,j}^{n,0} - z_{i,j}^{0,0})^2 \quad (10)$$

The global treatment ends with the global iteration m when:

$$\sum_{i,j \in D} (z_{i,j}^{n,m} - z_{i,j}^{0,m-1})^2 \leq Th_2 \quad (11)$$

4. Range finder by absorption

We report results from experiments using the differential light absorption (DLA) range finder technique which has been developed in our laboratory [1, 7]. This technique, which is well suited to small objects which may be immersed, derives range information from light absorption in a dispersive medium. The attenuation of light is a function of the thickness of the liquid over the object. Beer's law is used to relate the attenuation factor as a function of depth and liquid concentration. However, the intensity recorded is also affected by local surface orientations of the object. In order to eliminate this contribution and to recover a quantity which is a function of depth only, acquisitions are made at two distinct wavelengths, one in the liquid absorption range and the other in the infrared. The image taken in the infrared is not affected by the absorption of the liquid and can be considered as an ordinary intensity image. An image which is only affected by the absorption effect (hence range) is obtained by taking the ratio of the two images at these different wavelengths. The technique is very rapid and simple to implement. However the resulting range image tends to be fairly noisy since it is obtained by the division of two measured images.

5. Experiments

The fusion principle is applied here over the range image given by the DLA technique and the intensity image that is part of the process. For this to work properly, a measurement of the reflectance map is first performed by the intensity image of a sphere

A first example is shown in Figure 3. The two images at the top are intensity images taken at the two different wavelengths, the left one in the absorption range and the right one in the infrared. By combining these two intensity images, the DLA technique yields the corresponding range image shown bottom left. By using the experimental reflectance map measured previously and taking the infrared image as a bona fide intensity image, the range image is corrected to produce the much improved result shown bottom right. This result is obtained by setting $\alpha_1 = \alpha_2 = 0.1$, $\alpha_d = 0.2$ and $\alpha_p = 1.0$

A second example is presented in Figure 4. The object for this example is a cleft palate cast imprint. In the same way, the top images are the acquisition at the two different wavelengths and the images at the bottom show the range map before and after the fusion treatment.

The noise reduction that the method provides is difficult to evaluate for general object shapes because the true shape is generally unknown. However planar, cylindrical and spherical surface may be easily modeled and allow computing noise values. On selected objects that allow an easy surface modeling, the noise reduction has been evaluated.

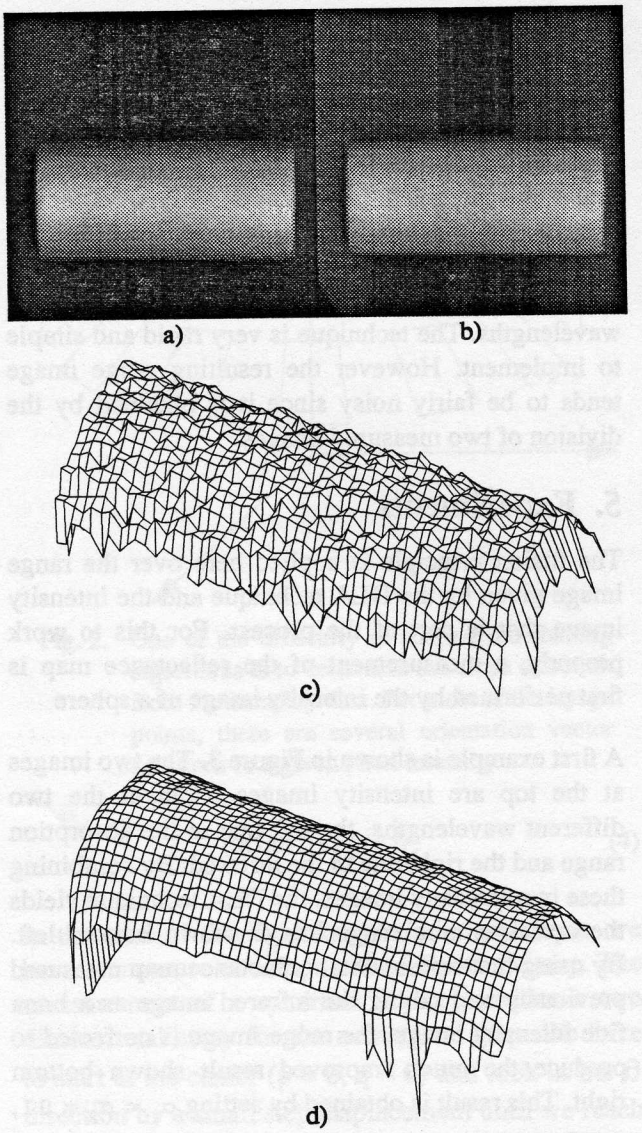

Fig. 3. An example of the application of the fusion algorithm on images from the differential light absorption technique. The object is a section of a cylinder. a) Intensity image taken in the absorption range. b) Intensity image taken in the infrared range (no absorption). c) Range image by combining a) and b). d) Range image resulting from the fusion of b) and c).

For planar surface, several noise reduction factors have been computed. The RMS noise reduction, for the DLA technique, has been found to vary between 2.19 and 3.24 by using a perfect reference plane fitted to the data each time.

6. Discussion and future work

The results obtained clearly support the advantages of fusing range and intensity data. With this technique, subsequent steps in the global vision process may be easier to perform. The method works well under reasonable acquisition conditions. As long as all parts of the object receive sufficient light and the dominant surface reflection lobe is the Lambertian one, the fusion method is applicable. The method is fairly robust unless there are very bad light conditions or the object has strong specular characteristics.

This paper has shown the application of the fusion method using the differential light absorption technique. The fusion method is quite general and can be readily adapted to other 3D acquisition systems without changing the described algorithms.

An effect that perturbs the recovered surface however is the possibility of multi-reflections, which tends to increase illuminance of points inside concave surfaces. This undesired effect produces erroneous slope vectors for points within concave regions. This perturbing effect is somewhat compensated by the observation that a point inside a concavity may not see all light sources and hence receives less light than the other points. This natural compensation is not sufficient however and the intensity observed inside a concavity is generally higher than expected.

7. Acknowledgments

The authors are grateful to Denis Laurendeau, Marielle Mokhtari, Michèle Aubin and Jean Côté for their help on the differential light absorption technique. Jean-François Méthot is supported by the Natural Sciences and Engineering Research Council of Canada. This project was supported, in part, by grant A5274 of the Natural Sciences and Engineering Research Council of Canada, and through funding provided by project A5 of the Institute for Robotics and Intelligent Systems of Canada.

8. References

[1] D. Laurendeau, R. Houde, M. Samson, D. Poussart, "*3-D Range Acquisition Through Differential Light*

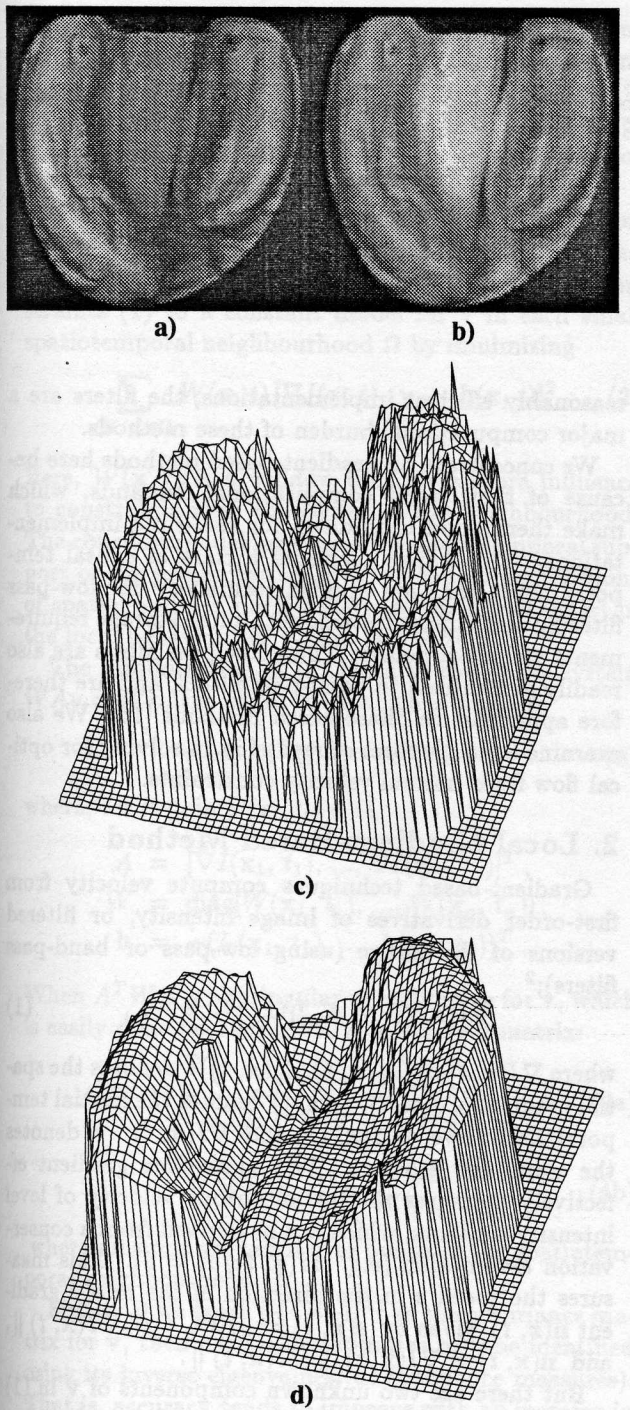

Fig. 4. An example of the application of the fusion algorithm on images from the differential light absorption technique. The object is a cleft palate cast imprint. a) Intensity image taken in the absorption range. b) Intensity image taken in the infrared range (no absorption). c) Range image computed by combining a) and b). d) Range image resulting from the fusion of b) and c).

Absorption," IEEE Transactions on Instrumentation and Measurement, vol. 41, no. 5, October 1992.

[2] R.C. Luo, M.G. Kay, "*Multisensor Integration and Fusion in Intelligent Systems,*" IEEE Transactions on Systems, Man and Cybernetics, vol. 19, no. 5, September/October 1989.

[3] D. Poussart, D. Laurendeau, "*3D Sensing for Industrial Computer Vision,*" in Advances in Machine Vision: Applications and Architectures, J. L. Sanz, Ed., Springer-Verlag, pp. 122-159, 1988.

[4] B.K.P. Horn, M.J. Brooks, "*Shape From Shading,*" Cambridge, MA, MIT Press 1989.

[5] Q. Zheng, R. Chellappa, "*Estimation of Illuminant Direction, Albedo, and Shape from Shading,*" IEEE Transactions on Pattern Analysis and Machine Intelligence, vol. 13, no. 7, July 1991.

[6] K. Ikeuchi, K. Sato, "*Determining Reflectance Properties of an Object Using Range and Brightness Images,*" IEEE Transactions on Pattern Analysis and Machine Intelligence, vol. 13, no. 11, November 1991

[7] D. Laurendeau, R. Houde, J. Cote, D. Poussart, "*3-D Range Acquisition Through Differential Light Absorption,*" Computer Vision and Digital Systems Laboratory, Laval University, Quebec (Quebec).

[8] T.A. Mancini, L.B. Wolff, "*3D Shape and Source Location from Depth and Reflectance,*" Proceedings of the IEEE Conference on Computer Vision and Pattern Recognition (CVPR), pp. 707-709, Champaign, Illinois, June 1992.

[9] J. G. Harris, "*A New Approach to Surface Reconstruction: The Coupled Depth/Slope Model,*" First International Conference on Computer Vision, pp. 277-283, London, England (1987).

[10] S. K. Nayar, K. Ikeuchi, T. Kanade, "*Shape from Interreflections,*" Third International Conference on Computer Vision, pp 2-11, (1990).